This is a repository copy of *Improving the hyperpolarization of (31)p nuclei by synthetic design*.

White Rose Research Online URL for this paper:
https://eprints.whiterose.ac.uk/90523/

Version: Submitted Version

Improving the Hyperpolarization of ^{31}P Nuclei by Synthetic Design

Michael J. Burns,[‡] Peter J. Rayner,[‡] Gary G. R. Green, Louise A. R. Highton, Ryan E. Mewis and Simon B. Duckett*

Centre for Hyperpolarization in Magnetic Resonance, Department of Chemistry, University of York, York, YO10 5NY

ABSTRACT: Traditional ^{31}P NMR or MRI measurements suffer from low sensitivity relative to ^{1}H detection and consequently require longer scan times. We show here that hyperpolarization of ^{31}P nuclei through reversible interactions with *para*hydrogen can deliver substantial signal enhancements in a range of regioisomeric phosphonate esters containing a heteroaromatic motif which were synthesized in order to identify the optimum molecular scaffold for polarization transfer. A 3588-fold ^{31}P signal enhancement (2.34% polarization) was returned for a partially deuterated pyridyl substituted phosphonate ester. This hyperpolarization level is sufficient to allow single scan ^{31}P MRI images of a phantom to be recorded at a 9.4 T observation field in seconds that have signal-to-noise ratios of up to 94.4 when the analyte concentration is 10 mM. In contrast, a 12 hour 2048 scan measurement under standard conditions yields a signal-to-noise ratio of just 11.4. ^{31}P-hyperpolarized images are also reported from a 7 T pre-clinical scanner.

Keywords: ^{31}P, NMR, MRI, *para*hydrogen, PHIP, SABRE

Phosphorus containing molecules are essential to the human body.[1-5] In addition, a number of widely prescribed pharmaceutical products contain one or more phosphorus atoms.[6-8] Due to ^{31}P's high natural abundance, coupled with a wide chemical shift range that is indicative of molecular environment, ^{31}P signal detection represents an exciting probe for magnetic resonance spectroscopy (MRS) and magnetic resonance imaging (MRI) studies in both inorganic chemistry and biochemistry. For example, recent studies have used ^{31}P MRS for the *in vivo* monitoring of metabolites in breast cancer,[9-10] liver disease,[11] schizophrenia[12] and tissue assessment.[13-14]

The detection of ^{31}P nuclei by magnetic resonance (MR), however, suffers from lower sensitivity than ^{1}H nuclei because of its lower magnetogyric ratio.[15] Consequently, high quality ^{31}P NMR spectra or MRI images require relatively large amounts of sample in conjunction with signal averaging. Hyperpolarization techniques are seen as a route to overcome this low sensitivity issue which arises from the small population difference (*ca.* 10^{-5}) that exists between the Zeeman-split energy levels that are probed. Until recently, ^{31}P hyperpolarization has received limited attention and the development of a simple method to achieve it is desirable.[16-17]

*Para*hydrogen induced polarization (PHIP) is a popular method of hyperpolarization that, utilizes molecular hydrogen as its source of polarization.[18-23] By incorporating p-H$_2$ into an unsaturated molecule its singlet symmetry is broken and this process unlocks it's latent, and normally invisible, polarization. A recent report using PHIP for ^{13}C detection, showed that labelled 1-^{13}C-

phospholactate-d_2 could be detected at just 5.74 mT.[24] PHIP has, however, been widely used to probe reaction mechanisms where it enables the detection of many metal hydride containing complexes.[25-27] In these studies magnetization transfer to ^{31}P has proven to be a very important feature of the characterization of many reaction products.[28]

A new form of PHIP, called Signal Amplification by Reversible Exchange (SABRE) has emerged as a tool for the rapid hyperpolarization of molecules without the need for changing their chemical identity.[29] SABRE utilizes a stable metal complex, such as [IrCl(COD)(IMes)] (**1**), (where IMes = 1,3-bis(2,4,6-trimethylphenyl)-imidazolium and COD = *cis, cis*-1,5-cyclooctadiene*)* to form what is known as the polarization transfer catalyst (Scheme 1).
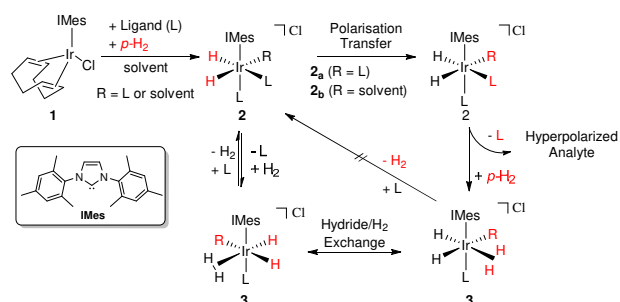
Scheme 1 An active SABRE catalyst can employ magnetic inequivalence (*e.g.* **2$_a$**) or chemical inequivalence (*e.g.* **2$_b$**) at the magnetization transfer stage. The generation of hyperpolarized ligands (**L**) that return to bulk solution through ligand exchange enables the production of analytes that are highly visible to NMR and MRI.

The role of catalyst **2** in Scheme 1 is to bring together p-H$_2$, now in the form of a pair of hydride ligands, and the hyperpolarization target (**L**). Polarization transfer cataly-

sis (PTC) occurs during the short time period for which **2** maintains this ligand arrangement. Polarization is passed through the *J*-coupling network of the metal complex into the ligand rather than by changing the chemical identity of the ligand through formal *p*-H$_2$ incorporation.[30] H$_2$ loss and rebinding of the analyte are necessary for the delivery of high levels of analyte hyperpolarization in conjunction with high catalyst turnover. In this case, the *p*-H$_2$ refresh step involves the short lived iridium dihydrogen dihydride complex **3**.[31]

To date, reported studies using the SABRE approach have focused on the polarization of ^{1}H[29, 32-34] and ^{13}C[29, 35] nuclei, although ^{15}N[36-37], ^{19}F[29] and ^{31}P[28, 38] signals have been seen when polarized. Both of the ^{31}P studies focused on PPh$_3$, with Zhivonitko *et al.* reporting that the signal for free PPh$_3$ can be enhanced by two orders of magnitude, and a single shot image recorded at 9.4 T.[38] Importantly, SABRE has been shown to be successful for a growing range of biologically relevant molecules; this has established the potential of the method to produce ^{1}H and ^{13}C hyperpolarized agents for subsequent MRI measurement.[29, 32, 35, 39-40]

Herein, we report the optimization of SABRE with respect to the hyperpolarization of ^{31}P nuclei within heteroaromatic molecules. We rationalize how the chemical structure affects the observed polarization level and thereby outline a strategy that may subsequently find use in the production of future diagnostic agents for ^{31}P MRI.

Materials and Methods

All reactions utilizing air- and moisture-sensitive reagents were performed in dried glassware under an atmosphere of dry nitrogen. Dry solvents (THF, toluene and DCM) were obtained from a Braun MB-SPS-800. For thin-layer chromatography (TLC) analysis, Merck pre-coated plates (silica gel 60 F254, Art 5715, 0.25 mm) were used. Column chromatography was performed on Fluka Silica gel (60 Å, 220-440 mesh). ^{1}H NMR, ^{13}C NMR and ^{31}P NMR spectra were measured on Bruker 400 MHz or 500 MHz spectrometers. Deuterated solvents (methanol-*d*$_4$ and chlorofrom-*d*) were obtained from Sigma-Aldrich and used as supplied.

The following compounds were synthesized according to literature procedures: **1**,[41] d$_{10}$-diethyl phosphite,[42] 4-pyridyl diphenylphosphine **L$_1$**,[43] 4-pyridyl diphenylphosphine oxide **L$_2$**,[44] 4-pyridylmethyl diethylphosphonate **L$_8$**, 3-pyridylmethyl diethylphosphonate **L$_9$**.[45] Detailed synthetic procedures and characterization data can be found in the supporting information.

p-H2 was produced by cooling H$_2$ gas over Fe$_2$O$_3$ at 30 K.[26] Samples involved the analysis of 5 mM concentrations of **1** and 5 or 6 eq. of substrate (**L$_1$-L$_{12}$**) in methanol-*d*$_4$ (0.6 or 3.0 mL) solution that was located in either a 5 or 8 mm NMR tube fitted with a J. Young's Tap. The resulting solutions were degassed prior to the introduction of *p*-H$_2$ at a pressure of 3 bar. Samples were then shaken for 10 s in a specified fringe field of either a 9.4 T Bruker Avance (III) NMR spectrometer or a 7 T Bruker BioSpec preclinical MRI scanner. They were then rapidly transported into the main magnetic field of the instrument for subsequent probing by NMR or MRI methods. The associated polarization transfer experiment data can be found in the supporting information.

Examining 4-substituted pyridine derivatives

Historically, *N*-heteroaromatic molecules have been shown to be excellent receptors for polarization transfer to ^{1}H and ^{13}C nuclei under SABRE.[29, 31, 33] We therefore synthesized a phosphine (**L$_1$**), a phosphine oxide (**L$_2$**), a phosphine sulfide (**L$_3$**) and a phosphonate ester (**L$_4$**) which incorporated a 4-substituted pyridine motif, as detailed in the supporting information (Figure 1). We selected the 4-substitution pattern for this study in order to minimize any steric interactions between the hyperpolarization target **L** and the IMes ligand in the catalyst **2**. We expected this restriction to promote activity in the widest range of analytes possible. A series of samples were then prepared in methanol-*d*$_4$ that contained **L$_1$-L$_4$**, at a concentration of 5 mM, and the catalyst precursor **1** at a 17% catalyst loading. These samples were probed after SABRE had taken place at 298 K on a 400 MHz NMR spectrometer by the application of a simple 90° *rf*. pulse. We will discuss the effects of SABRE on the pyridyl ^{1}H polarization, then the ^{31}P polarization and finally the polarization received by the other substituent groups.

When this 90° pulse was applied to the ^{1}H nuclei of these samples, only **L$_3$** proved to exhibit weak pyridyl proton polarization. The other three analytes produced good proton signal enhancements. For example, the two ^{1}H NMR signals of **L$_4$**, that were derived from the pyridine functionality, showed a 1499-fold total signal enhancement when the initial polarization transfer step was undertaken in a 45 G field. This high ^{1}H PTC was reflected in the fact that the corresponding ^{31}P signal exhibited a similarly impressive 545-fold signal enhancement. For ^{31}P, PTC was maximized through transfer at 0.5 G rather than the 45 G field observed for its ^{1}H nuclei. Figure 1 summarizes the corresponding ^{1}H and ^{31}P signal intensity gains determined for **L$_1$-L$_4$**.

L$_1$	L$_2$	L$_3$	L$_4$
^{1}H (45 G): 346	^{1}H (45 G): 219	^{1}H (45 G): 6	^{1}H (45 G): 1499
^{31}P (0.5 G): 57	^{31}P (0.5 G): 32	^{31}P (0.5 G): 6	^{31}P (0.5 G): 545

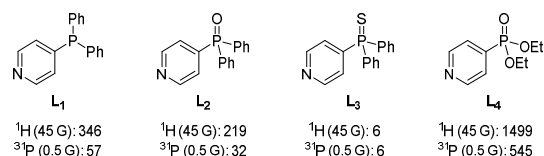**Figure 1** ^{1}H and ^{31}P signal intensity gains for analytes **L$_1$-L$_4$** under SABRE conditions using **1** as the catalyst.

A series of control experiments were then undertaken on triphenylphosphine, triphenylphosphine oxide and phenyldiethylphosphonate in order to explore the role that the pyridine substituent might play in the hyperpolarization transfer process. These experiments revealed that no polarization transfer took place into the ^{1}H or ^{31}P nuclei of these materials under the same SABRE conditions as used to hyperpolarize **L$_{1-4}$** described above. Based on this information it is clear that the pyridine motif is necessary for successful PTC under these conditions. This is achieved by the formation of an active SABRE catalyst as typified in Scheme 1. We note that this situation differs from that reported when the related [IrCl(H)$_2$(PPh$_3$)$_3$] complex was used to successfully polarize tri-

phenylphosphine at temperatures between 333 and 353 K by Koptyug et al..[38] In this case the Ir-P bond proved sufficiently labile that at elevated temperatures SABRE was successful. However, when **1** reacts with an excess of PPh$_3$ a series of new and rapidly relaxing hydride ligand signals are observed at δ -7.33, -7.98 and -8.59 which are indicative of the formation of [Ir(H)$_2$(H$_2$)(IMes)(PPh$_3$)$_2$]Cl. The formation of such as species precludes the observation of SABRE in these samples because of their role in the rapid quenching of p-H$_2$ (see Supporting Information).[46]

As a consequence of the formation of **2$_a$-L$_4$**, when the corresponding ^{1}H NMR spectra are examined under SABRE conditions polarized hydride resonances appear as a singlet in the region around δ –22.15 for the pair of chemically equivalent hydride ligands (see supporting information). Characteristic signals for **L$_4$**, as a ligand in **2$_a$-L$_4$**, are also seen to be polarized in the associated ^{31}P NMR spectra. We illustrate selected regions of these hyperpolarized ^{1}H and ^{31}P NMR spectra after PTC at 0.5 G, in Figures 2 and 3 respectively to detail some of these effects.

The hyperpolarized ^{1}H NMR trace shown in Figure 2 confirms that both of the two pairs of equivalent ring protons of bound **L$_4$** receive magnetization whilst those of the axial group remain unaffected. This is manifested in the detection of emission signals for the free analyte at δ 8.76, and for the equatorial ligand at δ 8.50. The magnetic state that produces this emission effect is single spin order in nature and associated with an enhanced but inverted Zeeman population.[47] In contrast, the corresponding pair of 3,5-ring protons in **L$_4$** produce anti-phase peaks that are separated by 13.5 Hz. This splitting corresponds to the value of $^3J_{PH}$ in **L$_4$** and requires that a heteronuclear two spin order proton phosphorus term is created through SABRE. Application of a 90° *rf*-pulse to the ^{1}H nuclei of this term creates the visible anti-phase signal that is seen; the creation of homonuclear proton terms of this type is a well-established characteristic of PHIP.[47] For **L$_4$**, the total ^{1}H signal enhancement was 1499-fold.
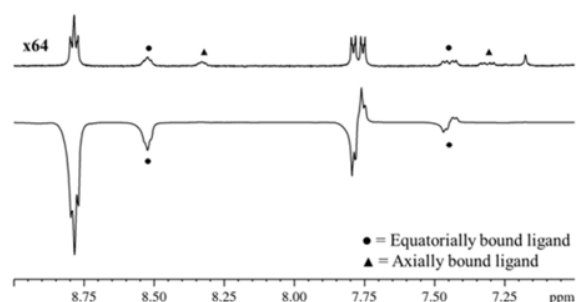

Figure 2 SABRE enhanced ^{1}H NMR spectrum (lower) and corresponding thermal reference spectrum (upper, x64 vertical expansion) of **2$_a$-L4** and **L$_4$** (● = equatorial ligand signal, ▲ = axial ligand signal of **2$_a$.L4**).

The hyperpolarized ^{31}P NMR spectrum of the **L$_4$** sample, collected as a single transient, also showed two anti-phase peaks, at δ 14.44 and 13.73 for free and equatorially-bound **L$_4$** respectively (Figure 3). The signal for free **L$_4$** showed a 545-fold increase in size after PTC at 0.5 G relative to the corresponding thermally polarized trace. The

separation between the point of maximum displacement and minimum displacement for the signal due to **L$_4$** in this NMR trace is 27.0 Hz (smaller $^4J_{PH}$ couplings are hidden within the peak envelope) and twice that of the separation shown in the ^{1}H NMR spectrum. This difference confirms the creation of proton-phosphorus two spin order term, which leads to a triplet when excited wherein the central feature has zero intensity (-1 : 0 : +1). Related behavior in PHIP derived trihydride complexes have been described previously.[25, 48-50] Application of the multinuclear OPSY protocol confirmed this deduction.[35, 51]
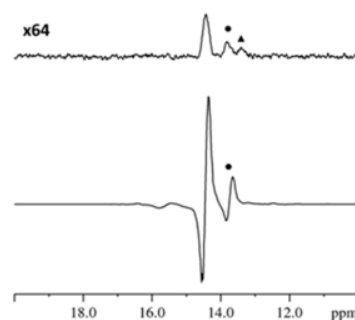

Figure 3 SABRE enhanced ^{31}P NMR spectrum (lower) and thermal reference spectrum (upper, x64 vertical expansion) of **2$_a$-L$_4$** and **L$_4$** (● = equatorial ligand, ▲ = axial ligand of **2$_a$-L$_4$**).

Interestingly, when **2a-L$_4$** is probed by EXSY methods both the axial and equatorial **L$_4$** ligands are observed to undergo exchange with the free ligand pool present in bulk solution. The exchange profile seen for axial-**L$_4$** suggests that there is some in-cage recombination of this ligand, a process which is not observed for equatorial-**L$_4$** (see supporting information). The axial ligand loss rate is 0.645 ± 0.010 s^{-1} at 283 K and slightly more rapid than equatorial ligand loss rate which is 0.522 ± 0.007 s^{-1}. The observed hyperpolarization seen in the equatorial-**L$_4$** ^{1}H and ^{31}P signals is therefore a consequence of SABRE prior to ligand loss.

We note that pyridylphosphonates find widespread use within a biological setting as lysophosphatidic acid receptor antagonists,[52-53] nucleotide analogues[54-55] and enzyme inhibitors.[56-57] Importantly, related compounds have been shown to exhibit low toxicity in rat studies (LD$_{50}$ of 3.2g/kg (oral)).[58] As a consequence of these facts and the observation that **L$_4$** delivers high levels of visible ^{31}P hyperpolarization we further optimized the ability of pyridylphosphonates to respond to PTC. This was achieved by the synthesis of the phosphonate derivatives **L$_5$-L$_{12}$** which are shown in Table 1, alongside the levels of ^{1}H and ^{31}P hyperpolarization that results from their analysis under SABRE.

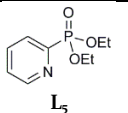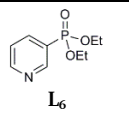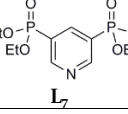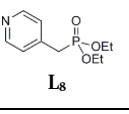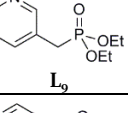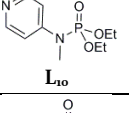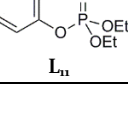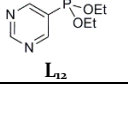| Substrate	^{1}H[a]	^{31}P[b]	Substrate	^{1}H[a]	^{31}P[b]
L5	2	0	**L6**	2866	336 (0.44)
L7	3689	860 (1.12)	**L8**	1353	48 (0.06)
L9	1174	39 (0.051)	**L10**	1005	60 (0.08)
L11	30	0	**L12**	224	87 (0.114)

Table 1 ^{1}H and ^{31}P NMR total signal intensity gains for **L5-L12** in a methanol-d_4 solution under 3 bar of p-H$_2$ achieved through PTC by **1** under SABRE in the specified magnetic field (for ^{31}P, % polarization indicated in brackets). 5 mM concentrations of **1** with 5 equivalents of **L7** and 6 of equivalents of **L5-L12** were employed at (a) 45 G and (b) 0.5 G.

Extension to 2 and 3 substitution

In order to examine the effect that the regiochemistry of substitution played on the polarization level we replaced the 4- substitution pattern exhibited by **L1-L4** with 2- and 3- substitutions in the form of substrates **L5** and **L6**. Polarization transfer into 2-pyridylphosphonate **L5** proved to be unsuccessful and this is due to the formation of a complex that yields a very broad hydride resonance at δ −31.3 which does not show PHIP. Upon cooling the solution to 233 K this hydride ligand signal separates into two resonances at δ −30.2 and δ −32.1 which confirms that this complex is a dihydride. The corresponding hydride ligand signals yield an average T$_1$ value of 0.56 s at 253 K and are therefore classically bonded and terminal in character.[46] Nonetheless, the presence of this complex in solution provides a pathway to rapidly destroy the p-H$_2$ present, presumably via the formation of a dihydrogen-dihydride complex, with the result that there is very little observable polarization transfer into **L5**.

In contrast, 3-substitution proved to result in good PTC. The measured ^{1}H signal enhancement at 45 G for **L6** was 2866-fold and the corresponding ^{31}P signal enhancement was 336-fold. Clearly, the change to a 3-substitution pattern has improved the level of ^{1}H PTC relative to 4-substitution but surprisingly decreased the efficiency for ^{31}P transfer. The synthesis of the *bis*-phosphonate **L7** was therefore undertaken, as this material contains two chemically equivalent ^{31}P nuclei, and one fewer pyridyl proton than the mono-substituted derivatives. We speculated that better ^{31}P-PTC might result as a consequence of this change on the basis that each p-H$_2$ molecule contains a specific amount of polarization and consequently when shared with fewer acceptor sites a net gain in the level of observable transfer might result. The corresponding ^{1}H and ^{31}P signal enhancements for **L7** were 2271 and 741-fold respectively when 6 equivalents of the analyte was employed and therefore this hypothesis is confirmed. However, one further and somewhat unexpected observation

was made, the enhanced steric bulk of **L7** results in a change in the active complex such that **2$_b$-L7** results wherein one coordination site is occupied by chloride (see supporting information). The two hydride signals for this complex appear at δ −23.74 and −24.06.[59] Because of this change in catalyst form we found that reducing the number of equivalents of **L7** to 5 led to an improvement in PTC, giving ^{1}H and ^{31}P signal enhancements of 3689 and 860-fold after transfer at 45 and 0.5 G respectively.

In order to further test the efficiency of polarization transfer to ^{31}P in these systems we added a series of spacers between the pyridyl carbon and the phosphorus center. In **L8** and **L9** this corresponds to the introduction of a -CH$_2$- group, while for **L10** it is -NMe- and for **L11** it is −O-. These analytes were SABRE active but while the pyridyl ring protons remained strongly enhanced the spacer acted to substantially reduce the levels of ^{31}P polarization. We also prepared a phosphonate using a pyrimidine motif (**L12**). This change again results in a reduction in the number of proton environments able to accept magnetization. While successful, the levels of both ^{1}H and ^{31}P signal enhancement were again lower than those achieved for the pyridylphosphonates.

We now address the potential of these substrates to act as MRI agents for which in-phase ^{31}P signals are desirable. As we have indicated, all of the described ^{31}P signals that were created through PTC in a 0.5 G appear in anti-phase. While this effect can be refocused to produce an in-phase signal, we proposed that changing the polarization transfer field (PTF) might achieve a similar result. This would be achieved by changing the relative proportions of single spin (in-phase) and two spin (anti-phase) components and result in a predominantly in-phase signal being obtained. A series of experiments were therefore performed in which the PTF was increased using a variable field polarizer[35] and the resulting ^{31}P signal monitored. We completed this process for both **L6** and **L7** (Figure 4). Significant in-phase contributions were observed after transfer at 45 G without any significant reduction in the overall ^{31}P
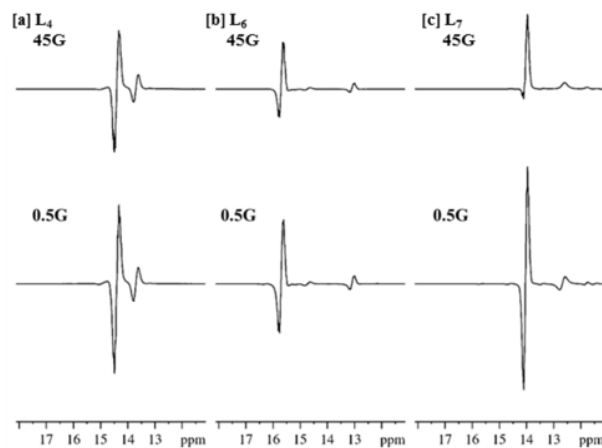

Figure 4 SABRE hyperpolarized ^{31}P NMR traces for **L4** [a], **L6** [b] and **L7** [c] that result after polarization transfer catalysis in a 45 G or 0.5 G field.

4

signal enhancement (216-fold vs. 336-fold for L_6 and 703-fold vs. 860-fold for L_7 at 45 G and 0.5 G respectively). While PTFs above 45 G did result in an increase in the relative single spin contribution, a sharp decline in the overall signal enhancement was noted. For L_6 the relative proportions of the single spin and two spin terms are 0.08:1 and 0.23:1 when the PTF is 0.5 G and 45 G respectively. In contrast, when L_7 is examined, the relative proportions are 0.06:1 at 0.5 G and 0.88:1 at 45 G respectively. We conclude from this that L_7 is potentially the better MRI probe for these model studies. This is because the signal for L_4 proved to remain predominately anti-phase at both 0.5 G (0.15:1) and 45 G (0.17:1) and it is therefore less suitable for such measurements.

Optimizing the level of ^{31}P hyperpolarization

Further examination of the hyperpolarized ^1H NMR spectra revealed that the signal enhancements described so far also extend into the ethyl groups of the phosphonate. Typically these ^1H signal enhancements were 50-fold per ethyl group and reflect a relayed ^1H-^{31}P-^1H transfer process. It was therefore reasoned that deuteration of the phosphonate ethyl esters would increase the level of retained ^{31}P polarization as transfer to ^2H is less efficient due to the large frequency difference that exists between them. Therefore we synthesized d_{10}-L_4, d_{10}-L_6 and d_{20}-L_7 and analyzed them under analogous conditions to their protio-counterparts (Figure 5). The levels of hyperpolarization seen in the aromatic proton signals of d_{10}-L_4, d_{10}-L_6 and d_{20}-L_7 proved to remain comparable to those of their protio analogues but the ^{31}P signals were found to dramat-
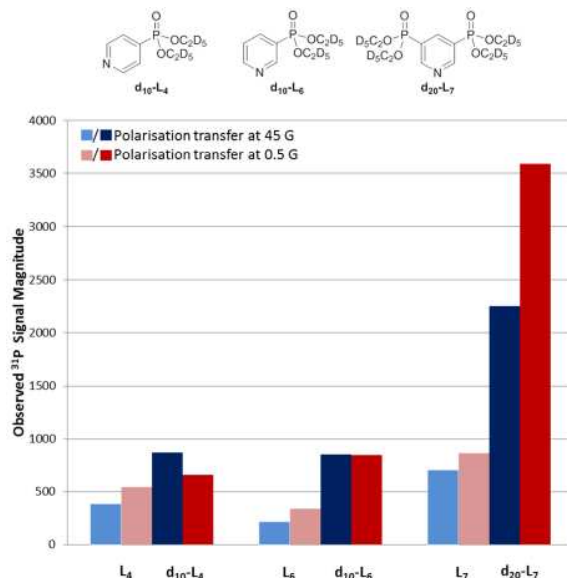

Figure 5 Structure of substrates d_{10}-L_4, d_{10}-L_6 and d_{20}-L_7 and their signal intensity gains, alongside those of their protio counterparts L_4, L_6 and L_7, under SABRE after PTC at the specified PTF.

ically increase in intensity.

Substrate d_{20}-L_7 yielded a ^{31}P signal gain of 3588 (2.3% polarization) after PTC at 0.5 G. A 2251-fold signal enhancement (1.4% polarization) is, however, achieved after PTC at 45 G with significant in-phase character being visible in the detected signal. We note this is an order of
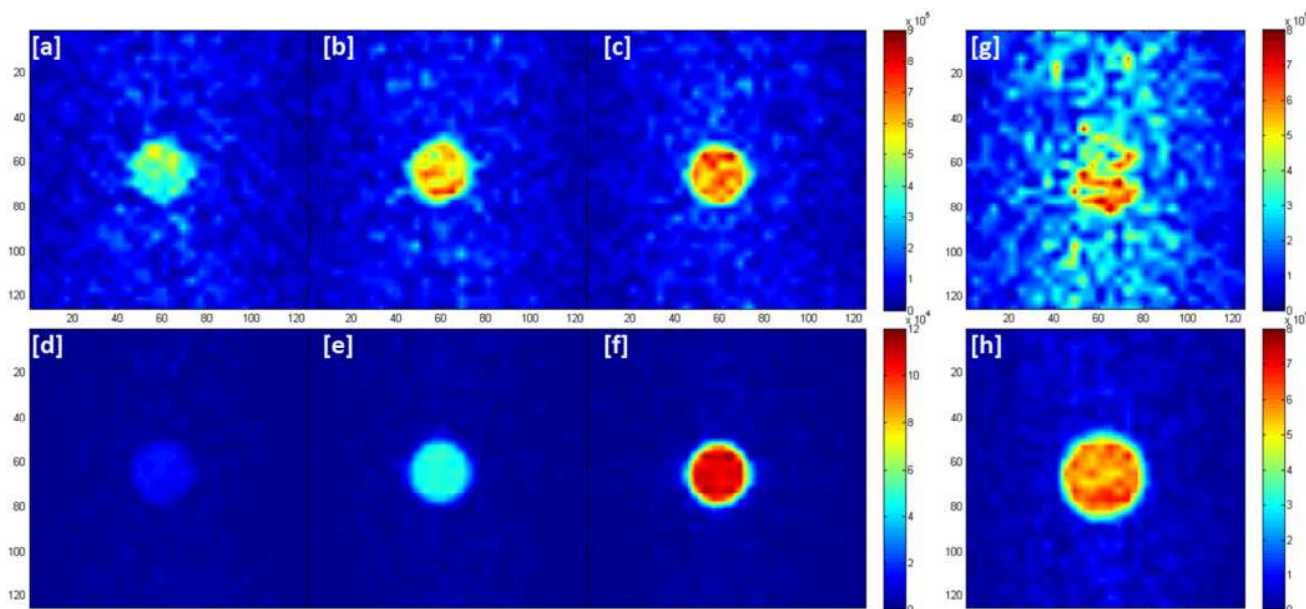
Figure 6 [a]-[c] Thermally polarized ^{31}P images of L_6, L_7 and d_{20}-L_7, respectively collected over 2048 averages. The flip angles used were 86° for L_6 and 90° for L_7 and d_{20}-L_7. The repetition time was 20 s. [d]-[f] Hyperpolarized images of L_6, L_7 and d_{20}-L_7, respectively collected in a single shot after PTC at 45 G. (TE/FOV/slice thickness were 3.2 ms/4 x 4 cm/5 mm respectively). [g] 2048-Average thermal image and [h] 1 scan hyperpolarized ^{31}P image of d_{20}-L_7 collected on a 7 T BioSpec 70/30 pre-clinical scanner. (TE/FOV/slice thickness were 12 ms/3 x 3 cm/10 mm respectively). Samples employed 5 mM concentrations of **1** in methanol-d_4 (3 mL) with L_6 (6 eq.), L_7 or d_{20}-L_7 (5 eq.) and 3 bar of p-H_2. SNR values were calculated by dividing the mean signal intensity value in the region with signal by the standard deviation of the residual signal seen in an analogously sized noise region.

magnitude larger than previously reported for ^{31}P enhancements using this technique and can be achieved without the need for elevated temperatures during the polarization transfer step.[38] In a further development, we completed the magnetization transfer by inserting the sample into a μ-magnetic shield, which attenuates the Earth's field by a factor of 3000-fold, prior to moving it into the 9.4 T magnet for examination. While this created in-phase ^{31}P magnetization,[30] the observed signal enhancement decreased to 381-fold (0.497%) under these conditions. It would therefore appear that simply changing the polarization transfer field to a readily accessible value between 0.5 and 130 G reflects the optimal route to achieve in-phase signal. We also note that complexes of type **1** are known to catalyze hydrogen-deuterium exchange[60] and as such, there is the potential to detect 1-proton-PHIP in such analytes.[61-62] Hence, we prepared a sample of **d$_{20}$-L$_7$** and **1** in methanol-d_4 under 3-bar of H$_2$ and followed it by ^{1}H NMR for a period of 10 days. At this point, 90% of the 2,6-protons had been replaced by deuterium. Subsequent SABRE catalysis led to a large reduction in the ^{31}P polarization transfer level. If the ^{31}P enhancements that were seen here were due to a 1-proton-PHIP, then the enhancement levels should remain comparable to those observed at day 1. This suggests that when such samples are examined they should be prepared shortly before their use.

Effect of relaxation on hyperpolarization level

We have thus far exemplified the ability to hyperpolarize ^{31}P and we next evaluated the spin-lattice relaxation times (T$_1$) of the analytes **L$_4$**, **d$_{10}$-L$_4$**, **L$_6$**, **d$_{10}$-L$_6$**, **L$_7$** and **d$_{20}$-L$_7$**. The T$_1$ relaxation values of the Zeeman based ^{31}P polarization are 8.3, 7.6, 9.2, 9.3, 5.3 and 6.0 s respectively in methanol-d_4. For **d$_{20}$-L$_7$** they increase to 6.5 seconds in ethanol-d_6 and decrease to 3.6 seconds in D$_2$O. These T$_1$ values, although short, do offer the opportunity to obtain images using the SABRE technique.

Imaging at high field

With a number of these substrates displaying favorable results we were hopeful that it would be possible to collect MRI with improved spatial resolution and short acquisition times. A series of hyperpolarized samples were therefore interrogated in a 9.4 T vertical bore scanner using the rapid acquisition with relaxation enhancement (RARE) pulse sequence. We employed an echo train length of 32 and a matrix size 32 x 32 with zero filling to 128 x 128. This resulted in a total single scan acquisition time of 500 ms. For comparison purposes, thermal images of **L$_6$**, **L$_7$** and **d$_{20}$-L$_7$** were recorded with 2048 averages, as shown in Figure 6. Under hyperpolarization conditions, the largest gains in signal-to-noise ratio (SNR) were observed for **d$_{20}$-L$_7$** (94.4) and reflected a >8-fold improvement on that of the thermal control (11.4). Improvements in SNR of >4-fold were also seen for **L$_7$**.

Similar images were also recorded on a 7 T BioSpec 70/30 pre-clinical scanner using **d$_{20}$-L$_7$** as the imaging agent (Figures 6g and 6h). A >6-fold improvement in SNR was achieved in the single scan hyperpolarized image (SNR = 27.7) when compared to the corresponding 2048-average thermal average (SNR = 4.5). We note that insertion of the sample tube into the horizontal scanner

caused more residual motion of the sample than was apparent in the analogous measurements on the vertical bore scanner. In addition, the time taken to transfer the sample to the magnet is *ca.* 5 s longer for the horizontal scanner and the magnetic fields experienced by the sample during transfer differ. A combination of these effects could account for the reduction in observed SNR that is observed in the hyperpolarized images that were recorded on the BioSpec. Nonetheless, these results confirm the value of these signal enhancements.

Conclusions

We have demonstrated that the ^{1}H and ^{31}P nuclei of a series of pyridyl substituted phosphonate esters, phosphine and phosphine oxide can be efficiently hyperpolarized using SABRE. Substitution at the 3-position delivered the greatest efficiency in polarization transfer catalysis to ^{1}H and ^{31}P, compared to substitution at the 2- and 4- positions. In the ligands that showed high performance, the phosphorus center was connected directly to the pyridyl ring such that a strong $^3J_{PH}$ coupling of 13.5 Hz exists between protons in the pyridyl ring and the ^{31}P nucleus.

The phosphonate esters used in this study contained ethyl substituents. These were shown to receive polarization *via* a relay mechanism which first polarized the pyridyl protons, then the ^{31}P nucleus and finally the ethyl protons. The net gain for the ethyl protons was of the order of 50-fold per ethyl group in comparison to the 2-3 thousand level shown by the aromatic protons. The effect of leakage of the ^{31}P magnetization to the ^{1}H nuclei of these ethyl groups was shown to reduce the level of retained ^{31}P polarization.

When the ^{1}H and ^{31}P polarization levels are compared between the protio forms of **L$_4$** and **L$_6$** and their deuterated ethyl counterparts **d$_{10}$-L$_4$** and **d$_{10}$-L$_6$** it could be seen that the best levels of ^{1}H polarization result for three-substituted **d$_{10}$-L$_6$**. Furthermore, the ^{31}P polarization levels are broadly similar for these two substrates at 1%. However, this raw observation masks the fact that for symmetrical **d$_{10}$-L$_4$** anti-phase signal dominates at all monitored polarization transfer fields. In addition, the T$_1$ values for **d$_{10}$-L$_4$** are much less than those for four-substituted **d$_{10}$-L$_6$** in the presence of **2**. The result of the small T$_1$ of **d$_{10}$-L$_4$** is that it must actually be better ^{31}P polarized under SABRE than **d$_{10}$-L$_6$**; we observe the magnetization *ca.* 3 seconds after polarization transfer has ceased and relaxation has reduced the hyperpolarized signal amplitude. These observations confirm that 3-substituted pyridines are more suitable candidates for the future rational design of MRI contrast agents that exploit SABRE. Deuterium incorporation into the ethyl groups has also been shown to increase the level of ^{31}P signal enhancement,

The symmetric *bis*-3-5-substituted derivative **L$_7$** was also synthesized, which proved to deliver strong ^{31}P polarization. We have shown that this is a consequence of more efficient transfer into the three remaining pyridyl protons, and that this synthetic strategy would enable the most atom efficient route to delivering such a pyridyl substituted agent. As a consequence, for **d$_{20}$-L$_7$**, the corresponding ^{31}P signal gain exceeds 3500-fold (2.3% polariza-

tion) which is an order of magnitude larger than that obtained using other approaches.[28, 38]

We also prepared systems where an C, N or O based spacer was introduced to separate the ^{1}H and ^{31}P functionalities. While the ^{1}H nuclei of the pyridyl groups in these analytes still retained high levels of hyperpolarization the level of transfer into the ^{31}P center was reduced by an order of magnitude. We concluded that the addition of a spacer was therefore undesirable.

In these studies, the process of SABRE was found to result in the creation of two types of ^{31}P hyperpolarization. These are single spin Zeeman magnetization and longitudinal two-spin heteronuclear H-P magnetization. When the corresponding terms were probed by a radio frequency pulse to ^{31}P they yield in-phase and anti-phase signals respectively. As an in-phase signal is desirable when investigating these hyperpolarized substrates using traditional MRI sequences we demonstrated that if the magnetic field experienced by the sample at the point of polarization transfer catalysis is 45 G, optimal in-phase ^{31}P signal enhancement results under SABRE in these systems. Interrogation of the resulting samples on a 9.4 T vertical bore scanner proved to allow images to be collected in a single scan at a 5 mM concentration. The SNR of a typical image was 94.4 and far exceeds that of a similar 12 hour measurement under normal conditions which employed 2048 averages. Although the T_1 values for these ^{31}P signals proved to be around 6 seconds, we have demonstrated that we can obtain good images on phantoms. We are working towards creating further phosphorus containing molecules that have longer T_1 values which might ultimately be used for *in vivo* applications. We expect that the methods of Levitt and Warren will be particularly relevant here.[63-67]

ASSOCIATED CONTENT

Supporting Information

Full synthetic procedures and spectroscopic data, NMR and MRI polarization transfer experiments, T_1 data and characterization data is available in the supporting information. This material is available free of charge *via* the Internet at http://pubs.acs.org.

AUTHOR INFORMATION

Corresponding Author

Correspondence should be addressed to simon.duckett@york.ac.uk

Author Contributions

‡These authors contributed equally.

Notes

The authors declare no competing financial interests.

ACKNOWLEDGMENT

REFERENCES

1.   Takeda, E.; Taketani, Y.; Sawada, N.; Sato, T.; Yamamoto, H., The Regulation and Function of Phosphate in the Human Body. *BioFactors* **2004**, *21*, 345-355.

2.   Wang, H.; Oster, G., Energy Transduction in the F1 Motor of Atp Synthase. *Nature* **1998**, *396*, 279-282.

3.   Boyer, P. D., The Atp Synthase - a Splendid Molecular Machine. *Annu. Rev. Biochem.* **1997**, *66*, 717-749.

4.   Hawthorne, J. N.; Pickard, M. R., Phospholipids in Synaptic Function. *J. Neurochem.* **1979**, *32*, 5-14.

5.   Dowhan, W., The Role of Phospholipids in Cell Function. In *Advances in Lipobiology*, Gross, R. W., Ed. Elsevier Science: 1997; Vol. 2, pp 79-107.

6.   Abdool Karim, Q., et al., Effectiveness and Safety of Tenofovir Gel, an Antiretroviral Microbicide, for the Prevention of Hiv Infection in Women. *Science* **2010**, *329*, 1168-1174.

7.   De Clercq, E., Acyclic Nucleoside Phosphonates: Past, Present and Future: Bridging Chemistry to Hiv, Hbv, Hcv, Hpv, Adeno-, Herpes-, and Poxvirus Infections: The Phosphonate Bridge. *Biochem. Pharmacol.* **2007**, *73*, 911-922.

8.   Reid, I. R., et al., Comparison of a Single Infusion of Zoledronic Acid with Risedronate for Paget's Disease. *N. Engl. J. Med.* **2005**, *353*, 898-908.

9.   Stehouwer, B. L.; Kemp, W. J. M.; Luijten, P. R.; Bosch, M. A. A. J.; Veldhuis, W. B.; Wijnen, J. P.; Klomp, D. W. J., 31P Magnetic Resonance Spectroscopy of the Breast and the Influence of the Menstrual Cycle. *Breast Can. Res. Treat.* **2014**, *144*, 583-589.

10.   Esmaeili, M.; Moestue, S. A.; Hamans, B. C.; Veltien, A.; Kristian, A.; Engebråten, O.; Mælandsmo, G. M.; Gribbestad, I. S.; Bathen, T. F.; Heerschap, A., In Vivo 31P Magnetic Resonance Spectroscopic Imaging (MRSI) for Metabolic Profiling of Human Breast Cancer Xenografts. *J. Mag. Res. Imag.* **2015**, *41*, 601-609.

11.   Chmelik, M.; Považan, M.; Krššák, M.; Gruber, S.; Tkačov, M.; Trattnig, S.; Bogner, W., In Vivo 31P Magnetic Resonance Spectroscopy of the Human Liver at 7 T: An Initial Experience. *NMR Biomed.* **2014**, *27*, 478-485.

12.   Nenadic, I.; Dietzek, M.; Langbein, K.; Rzanny, R.; Gussew, A.; Reichenbach, J. R.; Sauer, H.; Smesny, S., Effects of Olanzapine on 31P MRS Metabolic Markers in Schizophrenia. *Hum. Psychopham.: Clin. Expt.* **2013**, *28*, 91-93.

13.   Frey, M. A.; Michaud, M.; VanHouten, J. N.; Insogna, K. L.; Madri, J. A.; Barrett, S. E., Phosphorus-31 MMR of Hard and Soft Solids Using Quadratic Echo Line-Narrowing. *Proc. Nat. Acad. Sci.* **2012**, *109*, 5190-5195.

14.   Wu, Y.; Reese, T. G.; Cao, H.; Hrovat, M. I.; Toddes, S. P.; Lemdiasov, R. A.; Ackerman, J. L., Bone Mineral Imaged in Vivo by 31P Solid State Mri of Human Wrists. *J. Mag. Res. Imag.* **2011**, *34*, 623-633.

15.   Cady, E. B., In Vivo Cerebral 31P Magnetic Resonance Spectroscopy. *Neural Metabolism in Vivo*, Choi, I.-Y.; Gruetter, R., Eds. Springer US: New York, 2012; Vol. 4, pp 149-179.

16.   McCamey, D. R.; van Tol, J.; Morley, G. W.; Boehme, C., Fast Nuclear Spin Hyperpolarization of Phosphorus in Silicon. *Phys. Rev. Lett.* **2009**, *102*, 027601.

17.   Yang, A.; Steger, M.; Sekiguchi, T.; Thewalt, M. L. W.; Ladd, T. D.; Itoh, K. M.; Riemann, H.; Abrosimov, N. V.; Becker, P.; Pohl, H. J., Simultaneous Subsecond Hyperpolarization of the Nuclear and Electron Spins of Phosphorus in Silicon by Optical Pumping of Exciton Transitions. *Phys. Rev. Lett.* **2009**, *102*, 257401.

18.   Bonhoeffer, K. F.; Harteck, P., *Elektrochem. Angew. Phys. Chem.* **1986**, *35*, 621.

19.   Bowers, C. R.; Weitekamp, D. P., Transformation of Symmetrization Order to Nuclear-Spin Magnetization by

Chemical Reaction and Nuclear Magnetic Resonance. *Phys. Rev. Lett.* **1986**, *57*, 2645-2648.

20.   Bowers, C. R.; Weitekamp, D. P., Parahydrogen and Synthesis Allow Dramatically Enhanced Nuclear Alignment. *J. Am. Chem. Soc.* **1987**, *109*, 5541-5542.

21.   Morran, P. D.; Colebrooke, S. A.; Duckett, S. B.; Lohman, J. A. B.; Eisenberg, R., Reaction of Iodocarbonylbis(Trimethylphosphine)Rhodium(I) with Parahydrogen Leads to the Observation of Five Characterisable H2 Addition Products. *J. Chem. Soc., Dalt. Trans.* **1998**, 3363-3366.

22.   Eisenschmid, T. C.; Kirss, R. U.; Deutsch, P. P.; Hommeltoft, S. I.; Eisenberg, R.; Bargon, J.; Lawler, R. G.; Balch, A. L., Para Hydrogen Induced Polarization in Hydrogenation Reactions. *J. Am. Chem. Soc.* **1987**, *109*, 8089-8091.

23.   Green, R. A.; Adams, R. W.; Duckett, S. B.; Mewis, R. E.; Williamson, D. C.; Green, G. G. R., The Theory and Practice of Hyperpolarization in Magnetic Resonance Using Parahydrogen. *Prog. Nucl. Magn. Reson. Spectrosc.* **2012**, *67*, 1-48.

24.   Shchepin, R. V.; Coffey, A. M.; Waddell, K. W.; Chekmenev, E. Y., Parahydrogen Induced Polarization of 1-13c-Phospholactate-D2 for Biomedical Imaging with >30,000,000-Fold NMR Signal Enhancement in Water. *Anal. Chem.* **2014**, *86*, 5601-5605.

25.   Fox, D. J.; Duckett, S. B.; Flaschenriem, C.; Brennessel, W. W.; Schneider, J.; Gunay, A.; Eisenberg, R., A Model Iridium Hydroformylation System with the Large Bite Angle Ligand Xantphos: Reactivity with Parahydrogen and Implications for Hydroformylation Catalysis. *Inorg. Chem.* **2006**, *45*, 7197-7209.

26.   Godard, C.; Lopez-Serrano, J.; Galvez-Lopez, M. D.; Rosello-Merino, M.; Duckett, S. B.; Khazal, I.; Lledos, A.; Whitwood, A. C., Detection of Platinum Dihydride Bisphosphine Complexes and Studies of Their Reactivity through Para-Hydrogen-Enhanced Nmr Methods. *Magn. Reson. Chem.* **2008**, *46*, S107-S114.

27.   Giernoth, R.; Heinrich, H.; Adams, N. J.; Deeth, R. J.; Bargon, J.; Brown, J. M., Phip Detection of a Transient Rhodium Dihydride Intermediate in the Homogeneous Hydrogenation of Dehydroamino Acids. *J. Am. Chem. Soc.* **2000**, *122*, 12381-12382.

28.   Fekete, M.; Bayfield, O.; Duckett, S. B.; Hart, S.; Mewis, R. E.; Pridmore, N.; Rayner, P. J.; Whitwood, A., Iridium(III) Hydrido N-Heterocyclic Carbene–Phosphine Complexes as Catalysts in Magnetization Transfer Reactions. *Inorg. Chem.* **2013**, *52*, 13453-13461.

29.   Adams, R. W.; Aguilar, J. A.; Atkinson, K. D.; Cowley, M. J.; Elliott, P. I. P.; Duckett, S. B.; Green, G. G. R.; Khazal, I. G.; López-Serrano, J.; Williamson, D. C., Reversible Interactions with Para-Hydrogen Enhance Nmr Sensitivity by Polarization Transfer. *Science* **2009**, *323*, 1708-1711.

30.   Adams, R. W.; Duckett, S. B.; Green, R. A.; Williamson, D. C.; Green, G. G. R., A Theoretical Basis for Spontaneous Polarization Transfer in Non-Hydrogenative Parahydrogen-Induced Polarization. *The Journal of Chemical Physics* **2009**, *131*, 194505.

31.   Cowley, M. J.; Adams, R. W.; Atkinson, K. D.; Cockett, M. C. R.; Duckett, S. B.; Green, G. G. R.; Lohman, J. A. B.; Kerssebaum, R.; Kilgour, D.; Mewis, R. E., Iridium N-Heterocyclic Carbene Complexes as Efficient Catalysts for Magnetization Transfer from Para-Hydrogen. *J. Am. Chem. Soc.* **2011**, *133*, 6134-6137.

32.   Zeng, H., et al., Optimization of Sabre for Polarization of the Tuberculosis Drugs Pyrazinamide and Isoniazid. *J. Magn. Reson.* **2013**, *237*, 73-78.

33.   van Weerdenburg, B. J. A., et al., Ligand Effects of Nhc-Iridium Catalysts for Signal Amplification by Reversible

Exchange (Sabre). *Chem. Commun. (Cambridge, U. K.)* **2013**, *49*, 7388-7390.

34.   Eshuis, N.; Hermkens, N.; van Weerdenburg, B. J. A.; Feiters, M. C.; Rutjes, F. P. J. T.; Wijmenga, S. S.; Tessari, M., Toward Nanomolar Detection by Nmr through Sabre Hyperpolarization. *J. Am. Chem. Soc.* **2014**, *136*, 2695-2698.

35.   Mewis, R. E., et al., Probing Signal Amplification by Reversible Exchange Using an Nmr Flow System. *Magn. Reson. Chem.* **2014**, *52*, 358-369.

36.   Atkinson, K. D.; Cowley, M. J.; Elliott, P. I. P.; Duckett, S. B.; Green, G. G. R.; López-Serrano, J.; Whitwood, A. C., Spontaneous Transfer of Parahydrogen Derived Spin Order to Pyridine at Low Magnetic Field. *J. Am. Chem. Soc.* **2009**, *131*, 13362-13368.

37.   Theis, T.; Truong, M.; Coffey, A. M.; Chekmenev, E. Y.; Warren, W. S., Light-Sabre Enables Efficient in-Magnet Catalytic Hyperpolarization. *J. Magn. Reson.* **2014**, *248*, 23-26.

38.   Zhivonitko, V. V.; Skovpin, I. V.; Koptyug, I. V., Strong ^{31}P Nuclear Spin Hyperpolarization Produced Via Reversible Chemical Interaction with Parahydrogen. *Chem. Commun. (Cambridge, U. K.)* **2015**, *51*, 2506-2509.

39.   Hövener, J.-B., et al., Toward Biocompatible Nuclear Hyperpolarization Using Signal Amplification by Reversible Exchange: Quantitative in Situ Spectroscopy and High-Field Imaging. *Anal. Chem.* **2014**, *86*, 1767-1774.

40.   Dücker, E. B.; Kuhn, L. T.; Münnemann, K.; Griesinger, C., Similarity of Sabre Field Dependence in Chemically Different Substrates. *J. Magn. Reson.* **2012**, *214*, 159-165.

41.   Vazquez-Serrano, L. D.; Owens, B. T.; Buriak, J. M., The Search for New Hydrogenation Catalyst Motifs Based on N-Heterocyclic Carbene Ligands. *Inorg. Chim. Acta* **2006**, *359*, 2786-2797.

42.   Allen, K. J. H.; Nicholls-Allison, E. C.; Johnson, K. R. D.; Nirwan, R. S.; Berg, D. J.; Wester, D.; Twamley, B., Lanthanide Complexes of the Kläui Metalloligand, CpCo(P=O(OR)2)3: An Examination of Ligand Exchange Kinetics between Isotopomers by Electrospray Mass Spectrometry. *Inorg. Chem.* **2012**, *51*, 12436-12443.

43.   Weiner, M. A.; Schwartz, P., Cobalt(II) and Nickel(II) Complexes of Methyldiphenyl-4-Pyridylphosphonium Bromide. Effects of a Cationic Pyridyl Ligand. *Inorg. Chem.* **1975**, *14*, 1714-1716.

44.   Zhao, Y.-L.; Wu, G.-J.; Han, F.-S., Ni-Catalyzed Construction of C-P Bonds from Electron-Deficient Phenols Via the in Situ Aryl C-O Activation by Pybrop. *Chem. Commun. (Cambridge, U. K.)* **2012**, *48*, 5868-5870.

45.   Xue, J.; Diao, J.; Cai, G.; Deng, L.; Zheng, B.; Yao, Y.; Song, Y., Antimalarial and Structural Studies of Pyridine-Containing Inhibitors of 1-Deoxyxylulose-5-Phosphate Reductoisomerase. *Med. Chem. Let.* **2012**, *4*, 278-282.

46.   Kubas, G. J., Activation of Dihydrogen and Coordination of Molecular H-2 on Transition Metals. *J. Organomet. Chem.* **2014**, *751*, 33-49.

47.   Natterer, J.; Bargon, J., Parahydrogen Induced Polarization. *Prog. Nucl. Magn. Reson. Spectrosc.* **1997**, *31*, 293-315.

48.   Hasnip, S.; B. Duckett, S.; R. Taylor, D.; J. Taylor, M., Parahydrogen Enhanced Nmr Studies on Thermally and Photochemically Generated Products from [IrH3(CO)(PPh3)2]. *Chem. Commun. (Cambridge, U. K.)* **1998**, 923-924.

49.   Millar, S. P.; Zubris, D. L.; Bercaw, J. E.; Eisenberg, R., On the Mechanism of Dihydrogen Addition to Tantalocene Complexes. *J. Am. Chem. Soc.* **1998**, *120*, 5329-5330.

50.   Bregel, D. C.; Oldham, S. M.; Eisenberg, R., Mechanistic Studies on the Addition of Dihydrogen to Tantalocene Complexes. *J. Am. Chem. Soc.* **2002**, *124*, 13827-13832.

51.   Aguilar, J. A.; Elliott, P. I. P.; Lopez-Serrano, J.; Adams, R. W.; Duckett, S. B., Only Para-Hydrogen Spectroscopy (Opsy), a Technique for the Selective Observation of Para-Hydrogen Enhanced Nmr Signals. *Chem. Commun. (Cambridge, U. K.)* **2007**, 1183-1185.

52.   Heasley, B. H.; Jarosz, R.; Carter, K. M.; Jenny Van, S.; Lynch, K. R.; Macdonald, T. L., A Novel Series of 2-Pyridyl-Containing Compounds as Lysophosphatidic Acid Receptor Antagonists: Development of a Nonhydrolyzable Lpa3 Receptor-Selective Antagonist. *Bioorg. Med. Chem. Lett.* **2004**, *14*, 4069-4074.

53.   Heasley, B. H.; Jarosz, R.; Lynch, K. R.; Macdonald, T. L., Initial Structure–Activity Relationships of Lysophosphatidic Acid Receptor Antagonists: Discovery of a High-Affinity Lpa1/Lpa3 Receptor Antagonist. *Bioorg. Med. Chem. Lett.* **2004**, *14*, 2735-2740.

54.   Kers, A.; Stawiński, J., A New Type of Nucleotide Analogue with 4-Pyridylphosphonate Internucleotide Linkage. *Tetrahedron Lett.* **1999**, *40*, 4263-4266.

55.   Zmudzka, K.; Johansson, T.; Wojcik, M.; Janicka, M.; Nowak, M.; Stawinski, J.; Nawrot, B., Novel DNA Analogues with 2-, 3- and 4-Pyridylphosphonate Internucleotide Bonds: Synthesis and Hybridization Properties. *New J. Chem.* **2003**, *27*, 1698-1705.

56.   Sawa, M., et al., New Type of Metalloproteinase Inhibitor: Design and Synthesis of New Phosphonamide-Based Hydroxamic Acids. *J. Med. Chem.* **2002**, *45*, 919-929.

57.   Close, J., et al. Phosphorus Derivatives as Histone Deacetylase Inhibitors. WO/2008/010985, 16 Jul. 2007, 2008.

58.   Boenigk, W.; Hägele, G., Über Die Michaelis-Arbuzov-Reaktion Perhalogenierter Pyridine. *Chem. Ber.* **1983**, *116*, 2418-2425.

59.   Lloyd, L. S., et al., Hyperpolarisation through Reversible Interactions with Parahydrogen. *Catalysis Science & Technology* **2014**, *4*, 3544-3554.

60.   Cochrane, A. R.; Irvine, S.; Kerr, W. J.; Reid, M.; Andersson, S.; Nilsson, G. N., Application of Neutral Iridium(I) N-Heterocyclic Carbene Complexes in Ortho-Directed Hydrogen Isotope Exchange. *J. Lab. Comp. Radio.* **2013**, *56*, 451-454.

61.   Permin, A. B.; Eisenberg, R., One-Hydrogen Polarization in Hydroformylation Promoted by Platinum−Tin and Iridium Carbonyl Complexes: A New Type of Parahydrogen-Induced Effect. *J. Am. Chem. Soc.* **2002**, *124*, 12406-12407.

62.   Barskiy, D. A., et al., The Feasibility of Formation and Kinetics of Nmr Signal Amplification by Reversible Exchange (Sabre) at High Magnetic Field (9.4 T). *J. Am. Chem. Soc.* **2014**, *136*, 3322-3325.

63.   Pileio, G.; Bowen, S.; Laustsen, C.; Tayler, M. C. D.; Hill-Cousins, J. T.; Brown, L. J.; Brown, R. C. D.; Ardenkjaer-Larsen, J. H.; Levitt, M. H., Recycling and Imaging of Nuclear Singlet Hyperpolarization. *J. Am. Chem. Soc.* **2013**, *135*, 5084-5088.

64.   Feng, Y.; Theis, T.; Liang, X.; Wang, Q.; Zhou, P.; Warren, W. S., Storage of Hydrogen Spin Polarization in Long-Lived C-13(2) Singlet Order and Implications for Hyperpolarized Magnetic Resonance Imaging. *J. Am. Chem. Soc.* **2013**, *135*, 9632-9635.

65.   Tayler, M. C. D.; Levitt, M. H., Accessing Long-Lived Nuclear Spin Order by Isotope-Induced Symmetry Breaking. *J. Am. Chem. Soc.* **2013**, *135*, 2120-2123.

66.   Feng, Y.; Theis, T.; Wu, T. L.; Claytor, K.; Warren, W. S., Long-Lived Polarization Protected by Symmetry. *J. Chem. Phys.* **2014**, *141*.

67.   Stevanato, G.; Hill-Cousins, J. T.; Hakansson, P.; Roy, S. S.; Brown, L. J.; Brown, R. C. D.; Pileio, G.; Levitt, M. H., A Nuclear Singlet Lifetime of More Than One Hour in Room-Temperature Solution. *Angew. Chem., Int. Ed.* **2015**, *54*, 3740-3.